Plasma Physics and
Controlled Fusion

LETTER • OPEN ACCESS

High resolution measurements of core density collapse dynamics in LHD

To cite this article: R Sassella *et al* 2026 *Plasma Phys. Control. Fusion* **68** 062503

Plasma Physics and Controlled Fusion

OPEN ACCESS

RECEIVED
12 February 2026

REVISED
5 May 2026

ACCEPTED FOR PUBLICATION
19 May 2026

PUBLISHED
11 June 2026

LETTER

High resolution measurements of core density collapse dynamics in LHD

R Sassella[*], D J Den Hartog[1], A M Wright[1], Y Takemura[2], H Funaba[2], N Kenmochi[2], J Sarff[1], Y Suzuki[3], K Tanaka[2], H Uehara[2], H Yamaguchi[2] and R Yasuhara[2]

[1] University of Wisconsin-Madison, Madison, WI 53706, United States of America
[2] National Institute for Fusion Science, National Institutes of Natural Sciences, Toki 509-5292, Japan
[3] Graduate School of Advanced Science and Engineering, Hiroshima University, Higashi-Hiroshima 739-8527, Japan
[*] Author to whom any correspondence should be addressed.

E-mail: sassella@wisc.edu

Keywords: plasma confinement, collapse phenomena, LHD

Abstract

The core density collapse (CDC) is an abrupt instability that degrades the performance of super dense core stellarator plasmas on the Large Helical Device (LHD). In LHD, CDCs have proved to be an operational limit in so-called outward-shifted configurations. New measurements with high time resolution Thomson scattering characterize dynamics of the instability in the core. The density profile is observed to collapse inwards, narrowing the density peak till the core itself collapses. A hot, radially localized feature is also observed in the electron temperature profile during the collapse and disappears within a few hundred microseconds of CDC onset.

1. Introduction

High density operation offers a promising path towards achieving fusion in magnetically confined plasmas. Unlike tokamaks, which have a density limit proportional to plasma current (the Greenwald limit) [1], stellarators have no known hard density limit. The so-called Sudo density limit can cause stellarator discharges to terminate in radiative collapse, but this is a flexible limit that can be pushed with conditioning techniques like boronisation [2]. The lack of a hard density limit is one factor making high-density stellarator plasmas an appealing target for fusion scenario development [3, 4]. The Large Helical Device (LHD), a superconducting heliotron-type stellarator at the National Institute for Fusion Science in Toki, Japan, is capable of producing super-dense core (SDC) plasmas [5]. SDCs have a steep density gradient in the core plasma and a strongly peaked electron density profile up to $10^{21}\mathrm{m}^{-3}$[6]. LHD is a flexible device capable of producing discharges with a range of profile and stability properties. The location of the magnetic axis R_{ax}, fuelling method, and heating are some of the determining factors in discharge type. Super dense core plasmas must be produced in an 'outward-shifted' magnetic axis configuration in which the magnetic axis is set to $R > 3.7$ m [6]. SDCs are susceptible to a collapse phenomenon that can make core density and plasma stored energy drop by up to 50% [7]. This core density collapse (CDC) takes less than a millisecond [7]. Understanding the physical mechanisms of the CDC is crucial for predicting whether CDCs should be expected on other devices and whether they could represent a fundamental density limit in stellarators.

This Letter presents the first high resolution measurements of plasma temperature and density profiles during a CDC. A 20 kHz Thomson scattering diagnostic measured electron temperature and density profiles [8]. The new high-resolution data revealed that the density profile narrows before the innermost core collapses, suggesting that the collapse phenomenon propagates inward. The electron temperature profile has a short-lived and narrow region of markedly elevated temperature, which collapses along with the density. The pressure gradient increases before the core density drops. Similarities between these phenomena and simulations reported in the literature suggest that high-n edge mode/low-n core mode coupling and a widening stochastic region could be implicated as the collapse mechanism [9–12]. However, CDC simulations do not fully account for the T_e profile feature.

Because of the very dense plasma, some high time resolution diagnostics, such as electron cyclotron emission and fast charge exchange recombination spectroscopy, have not been able measure the dynamics of the collapse itself, and many diagnostics capable of measuring dense profiles, such as the 30 Hz Thomson scattering system, have not been fast enough to capture the $<$1 ms CDC event. Therefore, previous CDC experiments have focused on the prediction of CDC events and on the long term effect of the CDC on the plasma [7, 9]. Plasma is lost from the confinement region during a collapse, and the density profile does not recover even after equilibrium is re-established post-CDC [7]. Temperature, on the other hand, was not observed to be changed by the CDC in the long run [7]. In the millisecond before the CDC, 'precursor-like' fluctuations are often observed in low field side edge plasma line-integrated density [9]. This has led to a body of work exploring edge ballooning modes as the triggering mechanism for the CDC [10–13].

This letter is organized as follows. Section 2 lays out the conditions, discharge type, and the main diagnostics used in the experiment. Section 3 describes results. The focus is on millisecond-scale phenomena observed in the temperature and density profiles during a CDC event. Section 4 offers some discussion of the new results, including a comparison of measured pressure, temperature, and density profiles to CDC simulation literature, and a conclusion.

2. Experiment

To produce CDCs for this experiment, we targeted high outward-shifted SDC discharges. The magnetic axis was set to an outward-shifted configuration, $R = 3.85$ m. A vessel-mounted injector launched a sequence of hydrogen pellets into electron cyclotron heating-generated 'seed' plasma. With this technique, the frozen pellets ablate slightly as they pass through the relatively low density seed plasma, but deposit most of their density straight into the plasma core. The result is a radially peaked density profile with a large gradient around the core [6].

10 MW of continuous heating was applied with LHD's three tangential negative ion neutral beams, with an additional 4 MW of pulsed power from two diagnostic beams. NBI heating continued to increase plasma pressure even after pellet injection ended [6]. This setup produced super dense core plasmas that produced CDCs in most shots.

To resolve the sub-millisecond dynamics of the CDC, a fast Thomson scattering (FTS) system was employed [14]. The flashlamp-pumped Nd:YAG laser can produce a burst of 1 joule pulses at either 1 or 20 kHz, and fast switched-capacitor digitizers collect the data. The laser beam passes through the plasma at the midplane. Density and temperature measurements are collected from 70 radial locations, with a typical spatial separation $\sim$3 cm, building up detailed radial profiles. At 20 kHz, the FTS system has a 5 ms measurement window. SDC discharges have durations of hundreds of milliseconds, and CDC onset time and pellet injection time can both vary by tens of milliseconds. Consequently, timing the FTS system to capture the dynamics of the sub-millisecond CDC proved a significant challenge. The FTS trigger was set at a fixed time, and pellet timing was moderated to try to steer the CDC into the measurement window.

FTS density measurements are suitable for making qualitative inferences about changes to the evolving profile, but absolute calibration was not possible. The laser pulse energy of the FTS system was unstable early in the data collection window and the normal electron density (n_e) calibration coefficient could not be applied. As an alternative, the data was back-calibrated, taking advantage of the fact that the laser pulse instability was consistent from shot to shot. The back-calibration used a period of stable laser energy from a shot with no CDC. The density during this shot's FTS data collection was confirmed stable by checking the CO_2 laser interferometer. The interferometer measures density integrated over the path of the laser beam through the plasma, more concisely known as line-integrated density, or n_eL. n_eL in the core stays within 5% of the average during this 5 ms period. Of the total hundred frames of FTS data collected, the last thirty frames of FTS data, from the period with stable laser energy, were averaged together. This averaged stable profile was used to create a matrix of calibration factors to compensate for the early laser instability. Then the back-calibration matrix was applied to the CDC data captured by the FTS system, producing the density measurements shown in figures 3, 5, and 6. No back-calibration was required for FTS temperature measurements.

Other diagnostics include a slower cadence 30 Hz Thomson scattering system, a CO_2 heterodyne laser interferometer measuring line integrated density, and a suite of magnetic pickup coils, all of which collected data for the full duration each shot.

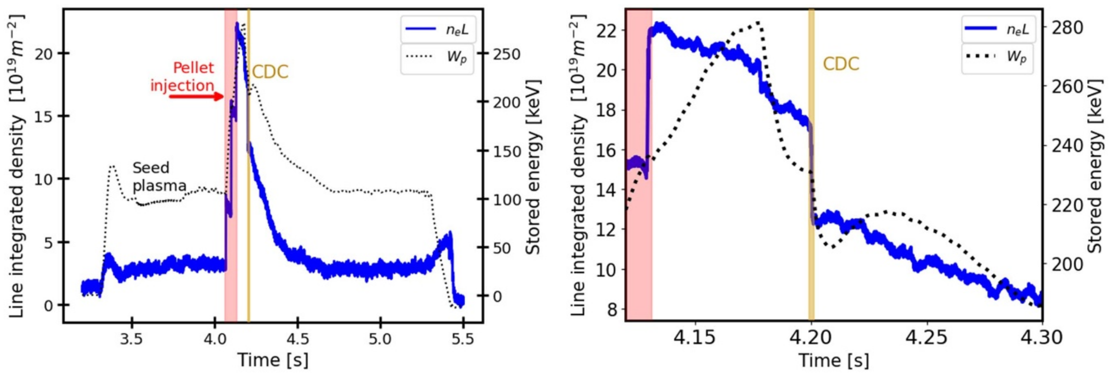

Figure 1. Time evolution of line integrated density and stored energy for a SDC discharge with a CDC at 4.200 s (#191 258). Rapid increases in n_eL are visible during the period of pellet injection (4–4.15 s). Both density and plasma stored energy increase with pellet injection, peak, and then begin to decrease gradually due to diffusion. The CDC (4.200 s) causes a sudden drop in plasma stored energy and line integrated density.

3. Results

We observed 23 super dense core plasmas with CDCs. Figure 1 shows the evolution of a typical CDC discharge (#191258). One radial chord of n_eL located in the plasma core is plotted. Plasma stored energy (W_p), measured with a diamagnetic loop, is also shown. n_eL and W_p start low with an ECH 'seed' plasma. Then n_eL steps up with each injected pellet. After pellet injection ends, particles gradually begin to diffuse and density starts to drop. Initially, temperature increases faster than density is lost, and pressure and stored energy continue to rise, peaking some tens of milliseconds after the end of pellet injection [6]. Then density loss overcomes heating, and pressure and stored energy both decline [5]. A sudden decrease in line integrated density and stored energy marks the CDC and loss of core confinement.

The FTS diagnostic took measurements from 4.200 to 4.205 s. In most cases the CDC fell outside the FTS measurement window, but in #191258, a CDC was captured in the FTS window. In other shots, plasma dynamics a few milliseconds before (#191266) or after (#191239, #191257, #191265) CDCs were recorded.

Thomson scattering measurements of the CDC show the density profile narrowing before the core collapses (figure 2). The peak density remains near its pre-CDC levels even as the peripheral regions of the core collapse. This plasma has a peak electron density (n_e) of just under $3 \times 10^{20}\mathrm{m}^{-3}$. The region of the plasma with $n_e > 2 \times 10^{20}\mathrm{m}^{-3}$ narrows from a width of ∼50 cm before the CDC to ∼15 cm in figure 2, which corresponds to a localization of the density peak during the CDC.

FTS measurements show the process of collapse in detail for the first time (see figure 3). The n_e profile is already narrowed compared to its post-fuelling, pre-CDC shape (shown on plot in light grey x's) when the first FTS data is collected at $t0 = 4.200\,009$ section Between the first profile and the second profile 170 μs later, peak core density stays high, while density further from the core begins to drop. This causes the density gradient to steepen. Core n_e has been notably affected by the time of the third profile, 379 μs, and has collapsed to its relaxed state 200 μs after that. At this point, the CDC is over and the profile has relaxed. The density profile changes very little for the remaining 4.5 ms of FTS data collection.

The evolution of the density profile suggests the collapse begins near the plasma edge. Because the peak density is affected last, the density gradient temporarily increases before the core collapses. The duration of the collapse of the peak density takes somewhere between 200 and 250 μs.

Another observation is a feature in the usually smooth electron temperature (T_e) profile (see figure 4). The feature consists of a narrow, hot region in the profile, about 30 cm wide and 30%–40% hotter than the neighbouring confined plasma. It takes place in the first half millisecond of the FTS data collection window, coinciding with the density changes described previously. The feature collapses within ∼250 μs. This T_e behaviour was only observed by FTS when a CDC was in the measurement window; CDC-free FTS measurements contained no notable T_e dynamics.

The T_e feature is already present at the start of the FTS data collection window. The last measurement before FTS with the 30 Hz Thomson system is 33 ms before FTS data collection begins, and shows a smooth, gently peaked profile with a maximum temperature around that of the T_e profile after the CDC (see figure 4). FTS and 30 Hz Thomson data from shots with CDCs just after (2–12 ms) the FTS

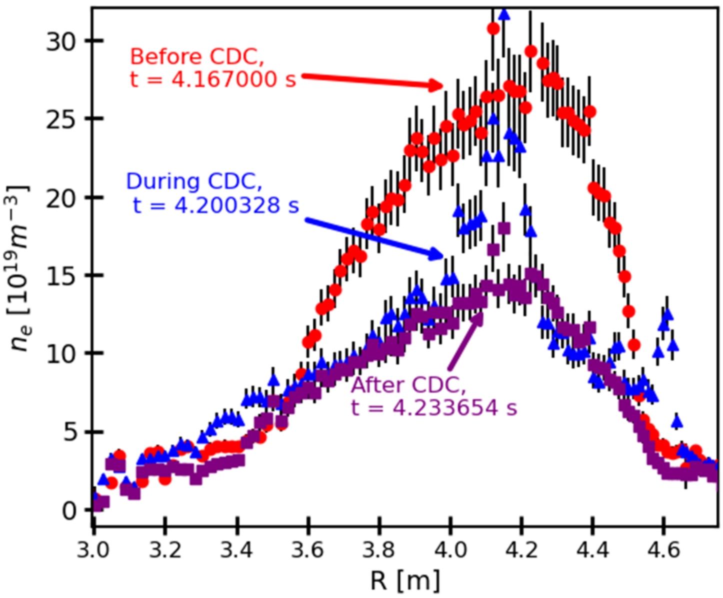

Figure 2. 30 Hz Thomson scattering measurements show the density profile collapsing from outer flux surfaces in. The innermost core density remains elevated as the profile peak narrows.

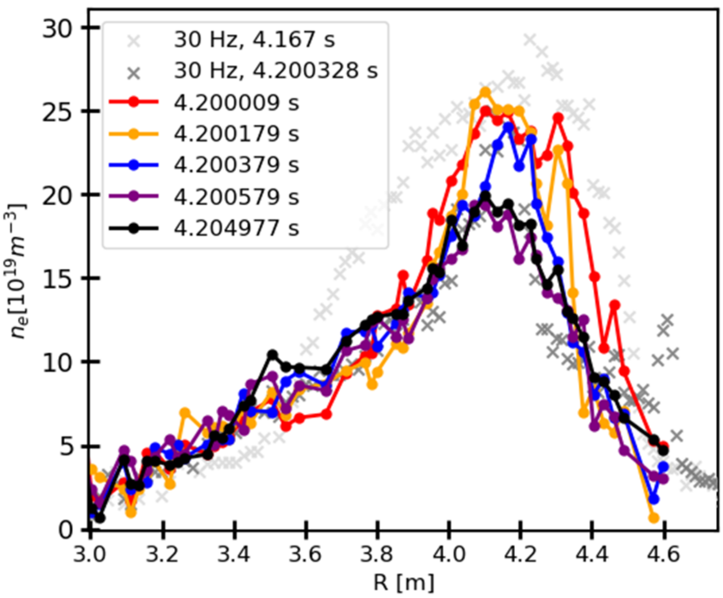

Figure 3. Fast Thomson scattering system measurements of density profile evolution during the core collapse. The first profile is collected at time t0 = 4.200 009 s; other timings are relative to that first profile. This first FTS profile (red line) is already narrowing as the CDC approaches; this is clear when comparing it to the 30 Hz n_e profile measurement 32 ms prior (light grey x's). For the first 170 μs, the density profile keeps narrowing without much density loss in the core. Slightly before 370 μs, the core density starts to decline; the profile continues to narrow. By 570 μs, the collapse is over, and the density profile remains relatively static for the next 4.5 ms of FTS data collection. A single profile was measured during this time window with 30 Hz Thomson scattering; slight discrepancies in profile shape between 30 Hz and fast Thomson measurements are observable around 4.3 m. This may be due to the described back-calibration process.

window do not show a similar T_e feature. Measurements including the first appearance and development of the T_e feature would be desirable for a thorough understanding of the feature.

After the collapse of the T_e spike, the profile reverts to a shape slightly flatter than the T_e profile 33 ms before the CDC. It maintains approximately this shape for the remaining 4.5 ms in the FTS data collection window, although the core temperature can be seen increasing slowly after the CDC. This reheat process could explain why previous studies without FTS capability [7, 9] reported no significant T_e changes associated with the CDC.

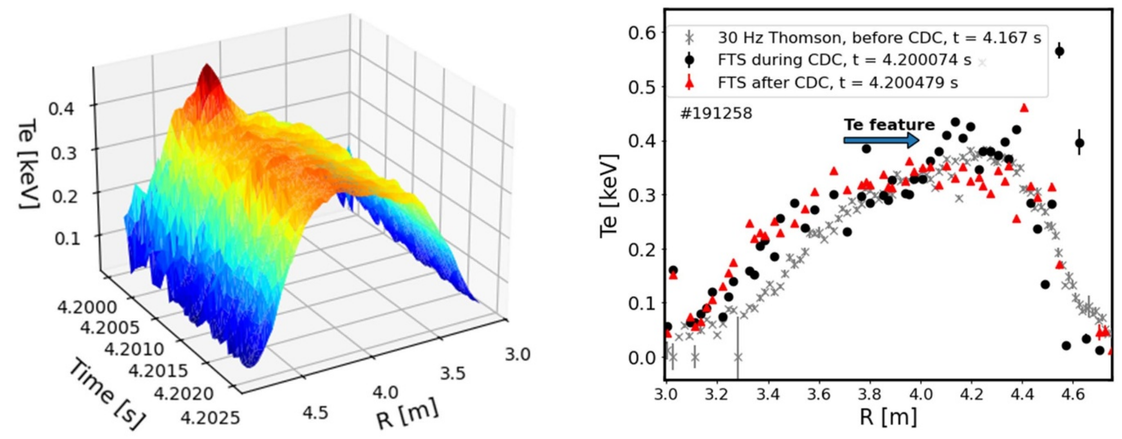

Figure 4. Evolution of the electron temperature profile during a CDC, captured with the 20 kHz Thomson scattering system (shot num. 191258). A narrow region of elevated T_e is visible in the plasma core at ∼4.2 m before it drops suddenly. Sample profiles from during and after the CDC show that the post-collapse profile shape is close to last pre-CDC T_e profile measurement made with 30 Hz Thomson. In the left-hand figure, the feature is visible as a red peak at the beginning of the collected data. In the right-hand figure, the feature is marked with a blue arrow.

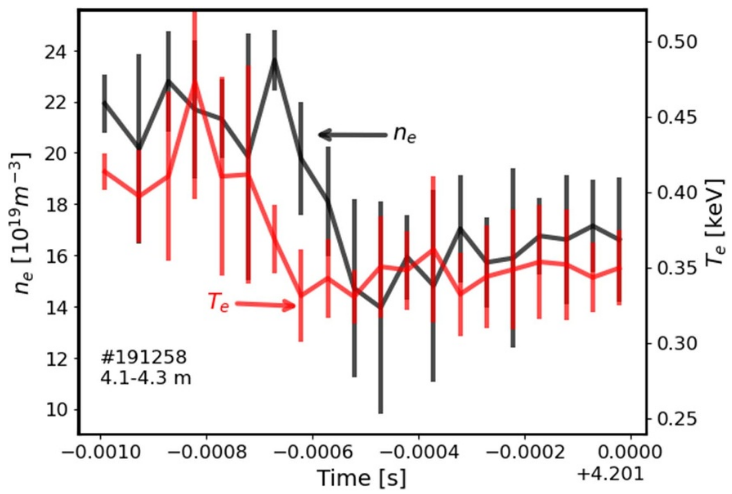

Figure 5. Temperature and density averaged over the core plasma, evolving through core collapse. Error bars are the standard deviation of the radially-averaged quantities.

The T_e feature coincides in radius with the narrowed n_e peak, centering at approximately 4.2 m. Figure 5 compares the dynamics of temperature and density in this radial region during the CDC. While T_e and n_e profiles display significant radial variation, their character within the core density peak region is more consistent. In order to focus on the time-varying behaviour of the temperature and density in the core, measurements of n_e and T_e were averaged over the core region, $R = 4.1$–4.3 m. Error bars show the standard deviation of the radial averaging. The early data shows the electron temperature feature as an elevated T_e. It starts to collapse a little before 4.2003 s, and has fully collapsed by about 4.2004 s. n_e, on the other hand, seems to start falling around 4.2004 s. T_e and n_e activity overlap in time, but the T_e feature collapses slightly ($\sim 100\ \mu$s) before the n_e profile does.

Density, temperature, and pressure profile evolution measurements made with FTS are summarized in figure 6.

Photon statistics are a source of error for both T_e and n_e measurements. Thomson scattering diagnostics inject laser light into the plasma. The scattering of this light by free electrons carries information about temperature and density. This photon-electron reaction has a low cross-section, meaning that only a small fraction of injected laser light results in Thomson scattering. The signal-to-noise ratio of Thomson scattering is consequently low, resulting in a statistical error that often dominates other error sources. The statistical error for the FTS system was estimated by comparing the variation between profiles measured at consecutive laser pulses/ time points. This profile-to-profile variation is on the order of

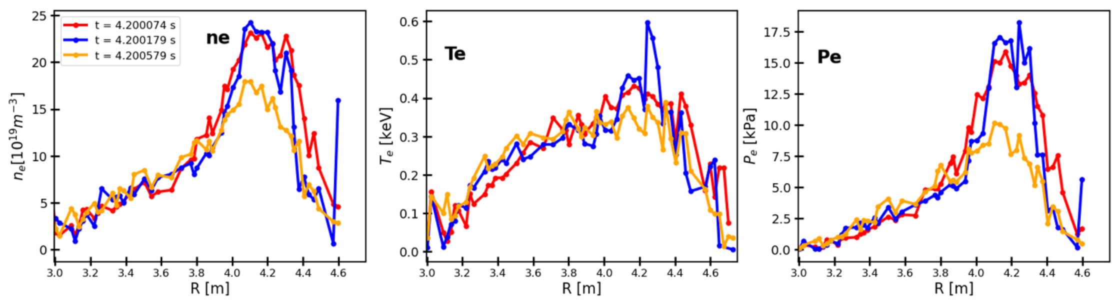

Figure 6. Radial profiles of electron density, temperature, and pressure, captured early, during, and at the end of CDC. Novel features of the CDC are most easily seen in the $t = 4.200179$ s profile.

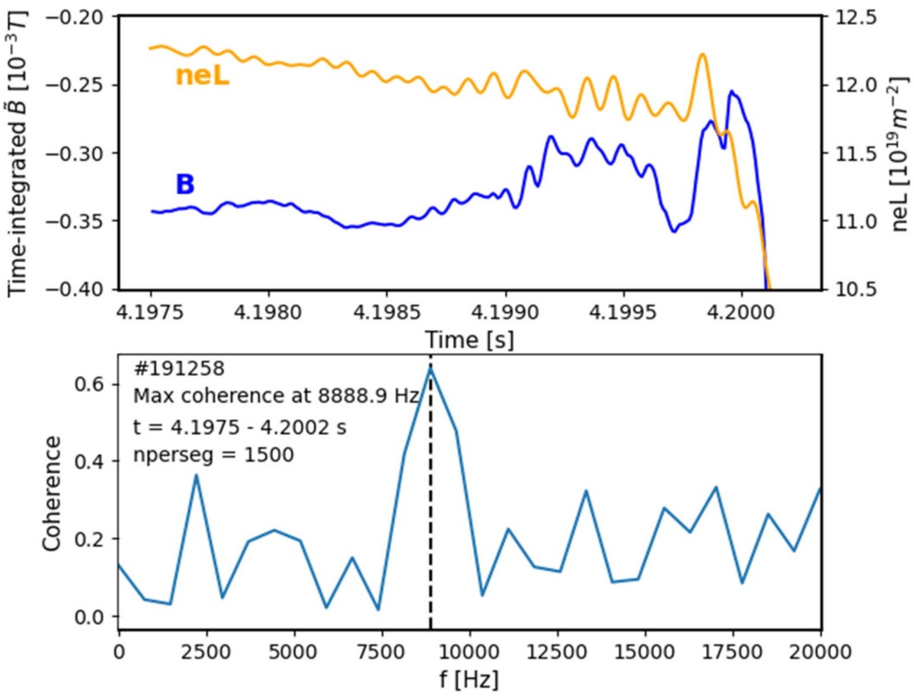

Figure 7. Precursor fluctuations in outboard line integrated density and magnetic field measured just inside the vessel appear around 4.199 s, about a millisecond before CDC onset. The field data comes from a pickup coil that produces a signal proportional to $\frac{dB}{dt}$ and so has been time-integrated. These signals have strong coherence around 9 kHz.

3% for T_e and 4% for n_e. An additional absolute error of 20–30 eV (about 4%–7% of the pre CDC core T_e) is expected on T_e measurements, but compared to statistical error, this should have little impact on analyses comparing relative changes in profile shapes.

Magnetic activity measured with a pickup coil on the vessel wall increased in the millisecond before CDC onset (see figure 7). While precursors in outboard chords of the CO_2 laser interferometer are well-documented in previous studies of the CDC [9], this is the first reported observation of a magnetic precursor. The decreased magnetic field strength of this experiment compared to past CDC studies may be responsible for the emergence of this phenomenon. The line integrated density and magnetic field in the millisecond before CDC have a coherence peak around 9 kHz.

4. Discussion and conclusions

Observations of density profile narrowing, T_e activity, and pressure profile steepening during the CDC are new, and the physical mechanisms behind them are not yet well-understood. However, parallels exist between some simulation predictions and the observed phenomena.

An extensive body of work has studied ballooning modes as a trigger for the CDC in LHD. Line-integrated density precursor activity observed in the outboard plasma just before CDCs may be the signature of the ballooning mode going unstable [9, 15]. Ideal MHD ballooning modes are pressure-driven instabilities localized to regions of bad curvature in LHD outward-shifted configurations [9, 13]. Nonlinear MHD simulations of CDCs predict that an unstable high toroidal mode number n ballooning mode in the plasma edge acts as the trigger for the CDC [10, 11]. The ballooning mode nonlinearly couples to and destabilizes a lower-n mode in the plasma core. A stochastic field region that starts narrow in the edge widens towards the core, as shown originally by Mizuguchi *et al* [10]. The models predict that the CDC occurs when the stochastic layer reaches the core [10–12].

Simulated predictions of field stochastization [10, 11] and density profile changes [11] agree with measurements of density profile narrowing. In the FTS measurements, n_e profile change during the CDC starts at the outer flux surfaces and propagates inwards (see figures 2 and 3). This results in a narrowing central peak, with the innermost core density remaining elevated until the final stage of the collapse. An inward-expanding stochastic region, like the one predicted in simulations of LHD [10–12, 16], could produce the observed density profile changes. Stochastic magnetic field lines can drive enhanced heat and particle transport. Previous CDC studies noted an increase in soft x-ray emission from the edge, which could reflect an edge-localized increase in electron temperature or density [9]. This emission could be the signature of an outflow of hot plasma from the core to the edge along stochastic field lines.

Temperature profile fluctuations during a CDC were also predicted by simulations performed by Civit-Bertran *et al* [11]. Performed in the visco-resistive MHD MIPS code [17] with equilibria made in HINT2 [18], the simulation models temperature, density, and pressure profiles before and during a CDC. As the field stochastizes and the instability saturates, both temperature and density profiles show increasing perturbation leading up to sudden core density loss. The T_e profile remains perturbed following the simulated CDC [11]. The MIPS simulation is the first theory work to predict temperature perturbations and heat loss during a CDC akin to the T_e profile changes newly observed with the FTS system. The simulated temperature profile also broadens inward after the CDC, consistent with both 30 Hz and FTS observations. However, unlike the observed T_e feature, the simulated temperature profile's perturbation is not a single, radially localized feature. Rather, the simulation predicts multiple large perturbations at radial locations spread broadly throughout the plasma. Additionally, while the T_e profile feature was observed to disappear during the CDC, simulated T_e perturbations persisted after the collapse [11].

Lacking observations of the feature's origin, two speculative scenarios have been envisioned. The feature could be the result of either rapid localized heating ('the spike scenario'), or it could be the last stages of the collapse of a flat, hot profile ('the collapse scenario'). The spike scenario would imply that some rapid, highly localized heating mechanism generates the feature. This aspect of the T_e feature remains an open question. In the collapse scenario, the flattish core T_e profile before the feature originates is as hot as the peak temperature of the feature. The broad, elevated temperature could come from NBI heating of the core plasma in the 33 ms between the 30 Hz Thomson measurement and the start of FTS data collection. In this scenario, the temperature profile collapses inwards, similar to the effect seen on the density profile, leaving the core T_e 'spike' to collapse last. This scenario is qualitatively similar to a T_e profile change and collapse observed in a simulation study of β limits by Wright and Ferraro [16]. These simulations, which used the extended-MHD code M3D-C1, showed that above a linear MHD stability threshold the T_e profile can collapse. If the heating is high enough, a small feature remains briefly elevated around the magnetic axis location before this, too, collapses. While the magnetic geometry and MHD properties of SDC plasmas are markedly different to those considered in the simulation (notably, SDCs are stable against interchange modes) this result suggests that nonlinear multi-mode coupling driving chaotic fields in the core can produce T_e profile features like the one observed with the FTS system during the CDC.

The FTS measured an increase in core pressure during the CDC. A FAR3D simulation by Varela *et al* likewise predicts an increase in pressure during the CDC and offers a possible explanation [12]. The enhanced pressure gradient in the simulation is a consequence of energy transfer from coupling between the high-n edge mode and the core. Low-n modes in the core are typically stable for SDC configurations [19], but the increased pressure gradient helps to destabilize these modes and stochastize the core [12].

The observation that the T_e feature collapses around 100 μs before the collapse of the core density is not predicted by simulations. This difference suggests heat transport is faster than particle transport. Stochastic magnetic transport is a possibility for such behaviour, since particle transport is constrained by ambipolarity. In any case, this observation clearly merits further investigation.

This paper presented the first high resolution measurements of temperature and density profiles during a sub-millisecond CDC event. Observations of density profile narrowing, T_e profile fluctuations, and pressure profile steepening were compared to CDC simulation literature. Inward propagation of the stochastic field region in simulation paralleled the observed density profile narrowing before and during the CDC and produced fluctuations in the predicted T_e profile. However, qualitative differences between measured and simulated T_e profile changes remain. Similarity between simulation and measurement suggests that these new high resolution observations of CDCs may be consistent with the ballooning mode trigger theory [10–13]. Open questions and discrepancies around the hot T_e feature and transport mechanisms of n_e and T_e remain to be resolved by future work.

Acknowledgments

This material is based upon work partially supported by the U.S. Department of Energy, Office of Science, Office of Fusion Energy Sciences, under Award Number DE-SC0026048. The Project was enabled by a allocation of runtime on LHD under the auspices of the NIFS-UW MoU and Task Agreement. R Sassella gratefully acknowledges travel support from the Department of Physics at UW-Madison, and valuable discussions with T Kinoshita and J Frazier.

Data availability statement

The data that support the findings of this study are openly available at the following URL/DOI:. https://doi.org/10.57451/lhd.analyzed-data [20].

ORCID iDs

R Sassella 0000-0002-4051-6517
D J Den Hartog 0000-0003-1667-2840
A M Wright 0000-0002-8852-3564
Y Takemura 0000-0003-3754-897X
H Funaba 0000-0003-2217-6018
N Kenmochi 0000-0003-1088-8237
J Sarff 0000-0001-8883-6678
Y Suzuki 0000-0001-7618-6305
K Tanaka 0000-0002-1606-3204
H Yamaguchi 0000-0002-1177-3370
R Yasuhara 0000-0001-5377-637X

References

[1] Greenwald M 2002 *Plasma Phys. Control. Fusion* **44** R27–R80
[2] Fuchert G *et al* 2020 *Nucl. Fusion* **60** 036020
[3] Anderson D, Canik J M, Hegna C C and Mowry C M 2025 *J. Plasma Phys.* **91** E65
[4] Lion J *et al* 2025 *Fusion Eng. Des.* **214** 114868
[5] Ohyabu N *et al* 2006 *Phys. Rev. Lett.* **97** 055002
[6] Sakamoto R *et al* 2010 *Fusion Sci. Techol.* **58** 53–60
[7] Ohdachi S *et al* 2010 *Contrib. Plasma Phys.* **50** 552–7
[8] Kenmochi N *et al* 2022 *Nat. Sci. Rep.* **12** 6979
[9] Ohdachi S *et al* 2017 *Nucl. Fusion* **57** 066042
[10] Mizuguchi N, Suzuki Y and Ohyabu N 2009 *Nucl. Fusion* **49** 095023
[11] Civit-Bertran A, Futatani S, Suzuki Y and Dominguez-Palacios J 2025 *Plasma Phys. Control. Fusion* **67** 085031
[12] Varela J *et al* 2026 *Nucl. Fusion* **66** 026017
[13] Varela J, Watanabe K Y, Nakajima N, Ohdachi S, Garcia L and Mier J A 2011 *Plasma Fusion Res.* **6** 1403013
[14] Funaba H *et al* 2022 *Nat. Sci. Rep.* **12** 15112
[15] Takeda K *et al* 2025 *Plasma Fusion Res.* **20** 1202037
[16] Wright A M and Ferraro N 2024 *Phys. Plasmas* **31** 102509
[17] Todo Y, Nakajima N, Sato M and Miura H 2010 *Plasma Fusion Res.* **5** S2062–2062
[18] Suzuki Y, Nakajima N, Watanabe K, Nakamura Y and Hayashi T 2006 *Nucl. Fusion* **46** L19
[19] Narushima Y *et al* 2009 *J. Plasma Fusion Res. Ser.* **8** 1070–4 (available at: https://www.jspf.or.jp/JPFRS/index_vol8.html)
[20] LHD Experimental Group 2002–2025 *LHD Analyzed Data Repository* (https://doi.org/10.57451/lhd.analyzed-data)